Supporting information

Fused tetracyclic tris[1,2,4]triazolo[1,3,5]triazine as a novel rigid electron acceptor for efficient thermally activated delayed fluorescence emitters

Suraj Kumar Pathak [a,b], Yepeng Xiang [c], Manli Huang [c], Taian Huang [a], Xiaosong Cao [a], He Liu [a*], Guohua Xie [c], Chuluo Yang [a,c*]

[a] *Guangdong Research Center for Interfacial Engineering of Functional Materials,Shenzhen Key Laboratory of Polymer Science and Technology, College of Materials Science and Engineering, Shenzhen University, Shenzhen 518060, P. R. China. liuhe001@szu.edu.cn, clyang@szu.edu.cn.*

[b] *Key Laboratory of Optoelectronic Devices and Systems of Ministry of Education and Guangdong Province, College of Optoelectronic Engineering, Shenzhen University, Shenzhen 518060*

[c] *Hubei Key Lab on Organic and Polymeric Optoelectronic Materials, Department of Chemistry, Wuhan University, Wuhan, 430072, P. R. China, clyang@whu.edu.cn*

General information

All oxygen- and moisture-sensitive manipulations were carried out under an inert atmosphere. All the chemicals were purchased from commercial sources and used as received unless stated otherwise. Toluene was refluxed over Na and distilled under dry argon. Synthesized compounds were subject to purification by temperature gradient sublimation in high vacuum before used in subsequent studies. The 500 MHz 1H and 125MHz ^{13}C NMR spectra were recorded on a Bruker Ascend 500 spectrometer using DMSO-D_6 as solvent and tetramethylsilane (TMS) as an internal reference. High-resolution electrospray (ESI) mass spectra were performed on SCIEX TripleTOF6600 nanoLCMS. UV-Vis absorption spectra were recorded on a Shimadzu UV-2700

recording spectrophotometer. Photoluminescence (PL) spectra were recorded on a Hitachi F-4600 fluorescence spectrophotometer. Phosphorescence spectra of thin films were conducted at 77K. Thermogravimetric analysis (TGA) was recorded on a TA Q50 instrument under nitrogen atmosphere at a heating rate of 10^{o}C/min from 25 to 800 ^{o}C.Thetemperature of degradation (T_d) was correlated to a 5% weight loss. Differential Scanning Calorimetry were carried out on a TA Q200. The glass transition temperature (T_g) was determined from the second heating scan at a heating rate of 10^{o}C min^{-1} from 25 to 250 ^{o}C. Cyclic voltammetry (CV) was carried out in acetonitrile (oxidation scan) at room temperature with a CHI voltammetric analyzer. Tetrabutylammoniumhexafluorophosphate (0.1 M) was used as the supporting electrolyte. The conventional three-electrode configuration consisted of a platinum working electrode, a platinum wire auxiliary electrode and an Ag wire pseudo-reference electrode with ferroceniumferrocene (Fc^+/Fc) as the internal standard. Cyclic voltammograms were obtained at scan rate of 100 mV/s. Formal potentials were calculated as the average of cyclic voltammetric anodic and cathodic peaks. The HOMO energy levels of the compounds were calculated according to the formula: -[4.8 + ($E_{1/2(ox/red)}$ - $E_{1/2(Fc/Fc+)}$)] eV. The onset potential was determined from the intersection of two tangents drawn at the rising and background current of the cyclic voltammogram. The PL lifetimes were measured by a single photon counting spectrometer from Edinburgh Instruments (FLS920) with a Picosecond Pulsed UV-LASTER (LASTER377) as the excitation source. The samples were placed in a vacuum cryostat chamber with the temperature control. The solid state absolute PLQYs were measured on a Quantaurus - QY measurement system (C9920-02, Hamamatsu Photonics) equipped with a calibrated integrating sphere in the host of CzSi (5 wt%) and all the samples were excited at 315 nm. During the PLQY measurements, the integrating sphere was purged with pure and dry argon to maintain an inert environment. The ground state

and excited states molecular structures were optimized at the B3LYP-D3(BJ)/def2-SVP and PBE0/def2-SVP respectively; the S1 and T1 geometries were optimized via time-dependent DFT (TDDFT) at the PBE0/def2-SVP.

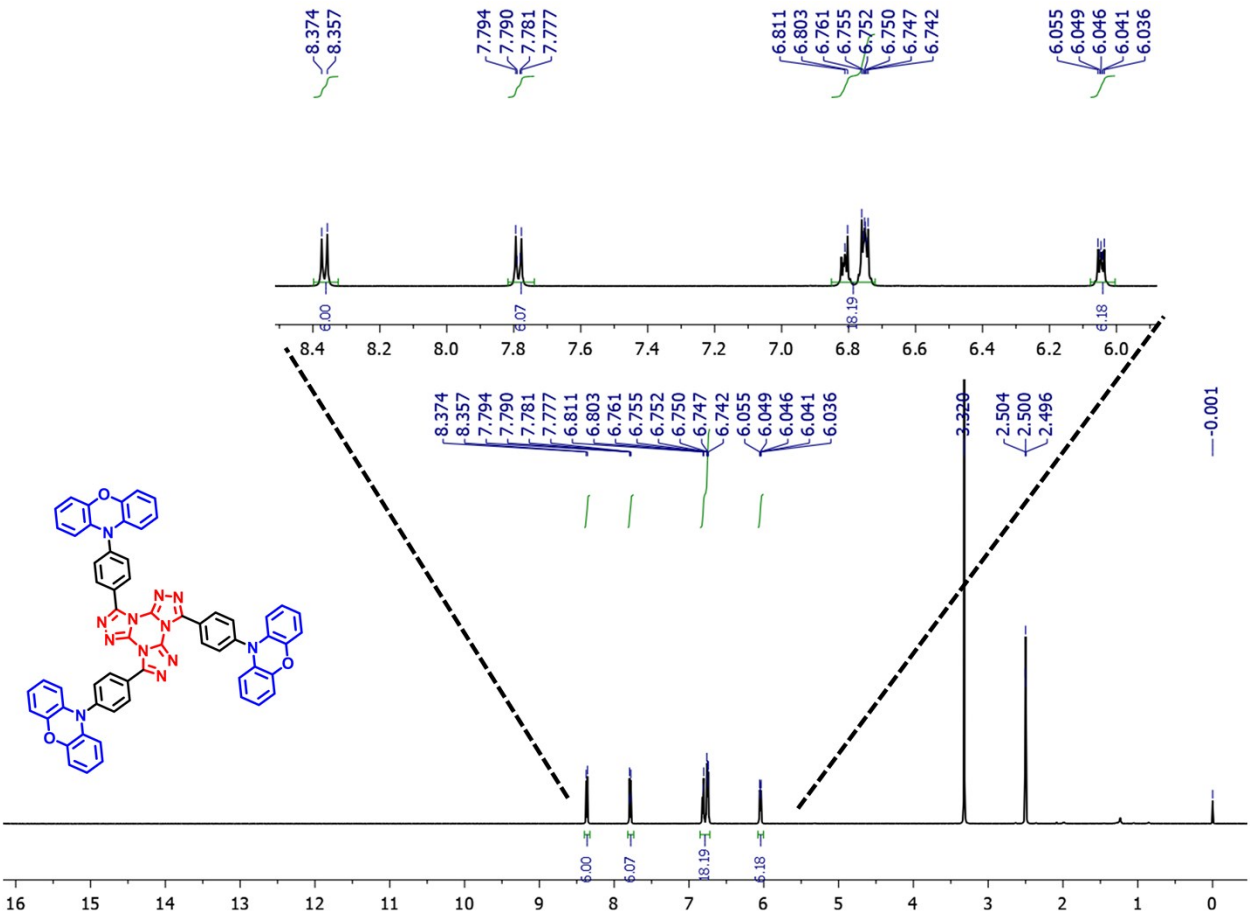

Figure S1. ^{1}H NMR spectrum of **TTT-PXZ** in DMSO-D_6 (500 MHz, 25 °C).

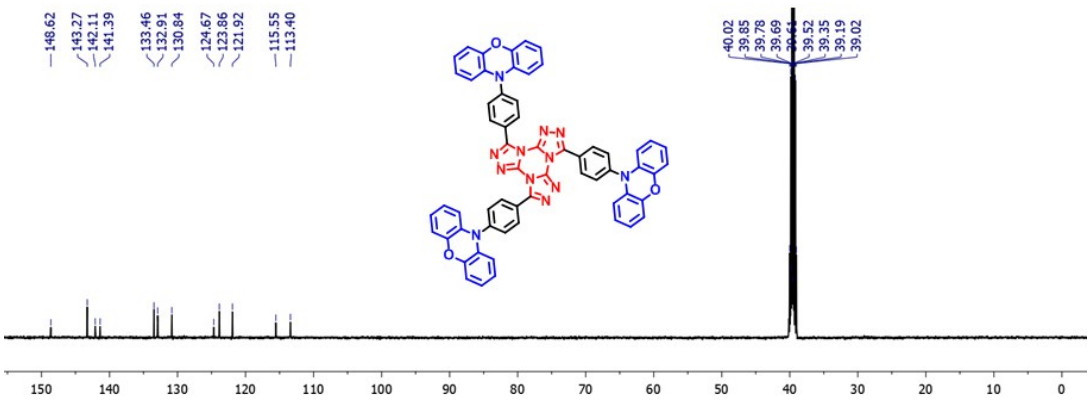

Figure S2. ^{13}C NMR spectrum of **TTT-PXZ** in DMSO-D_6 (125 MHz, 25 °C).

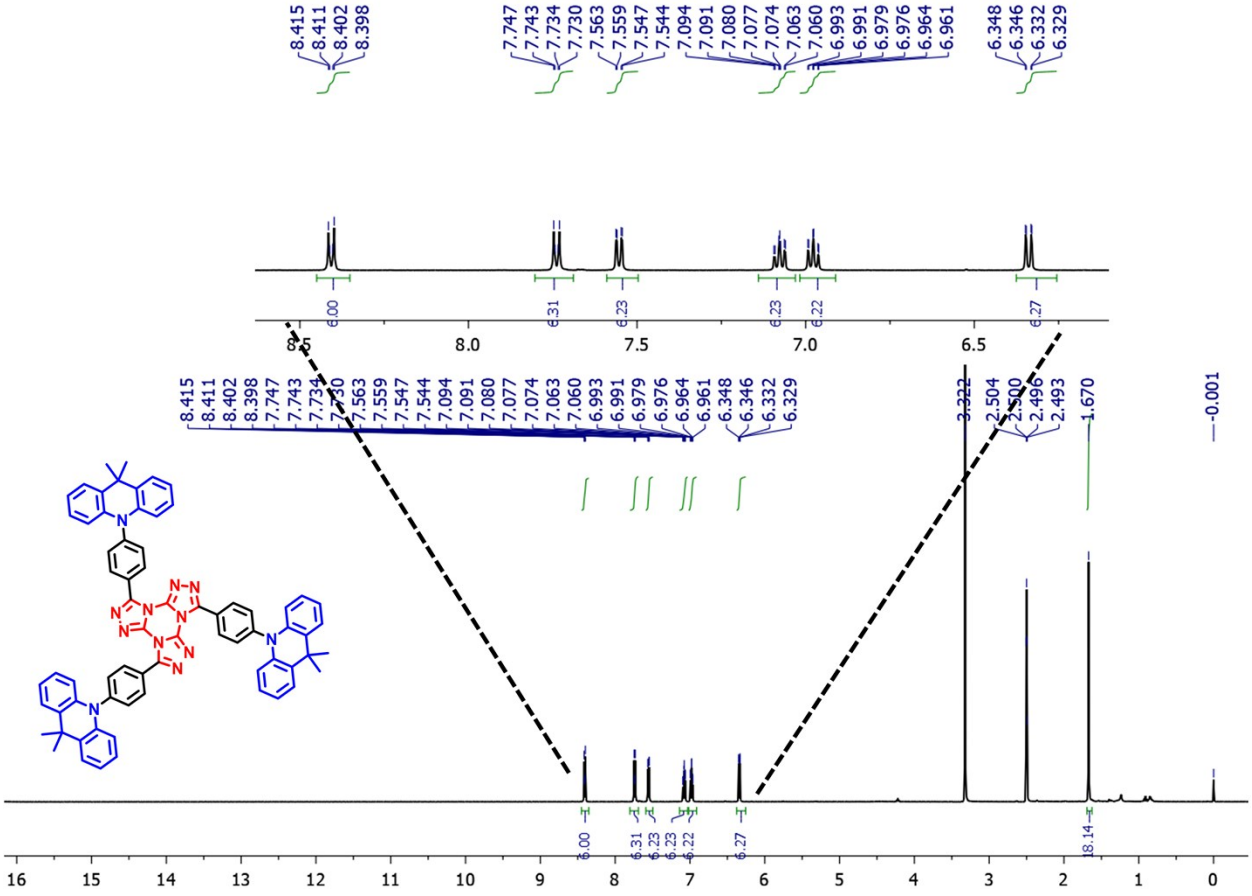

Figure S3. ^{1}H NMR spectrum of **TTT-DMAC** in DMSO-D_6 (500 MHz, 25 °C).

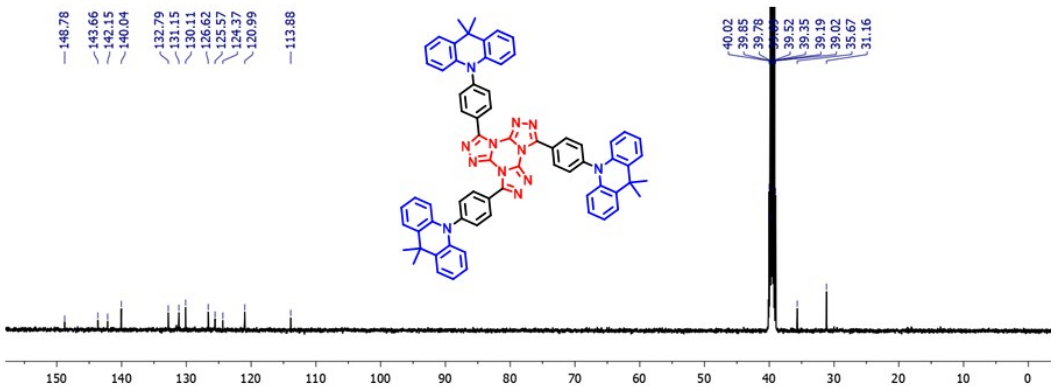

Figure S4. ^{13}C NMR spectrum of **TTT-DMAC** in DMSO-D_6 (125 MHz, 25 °C).

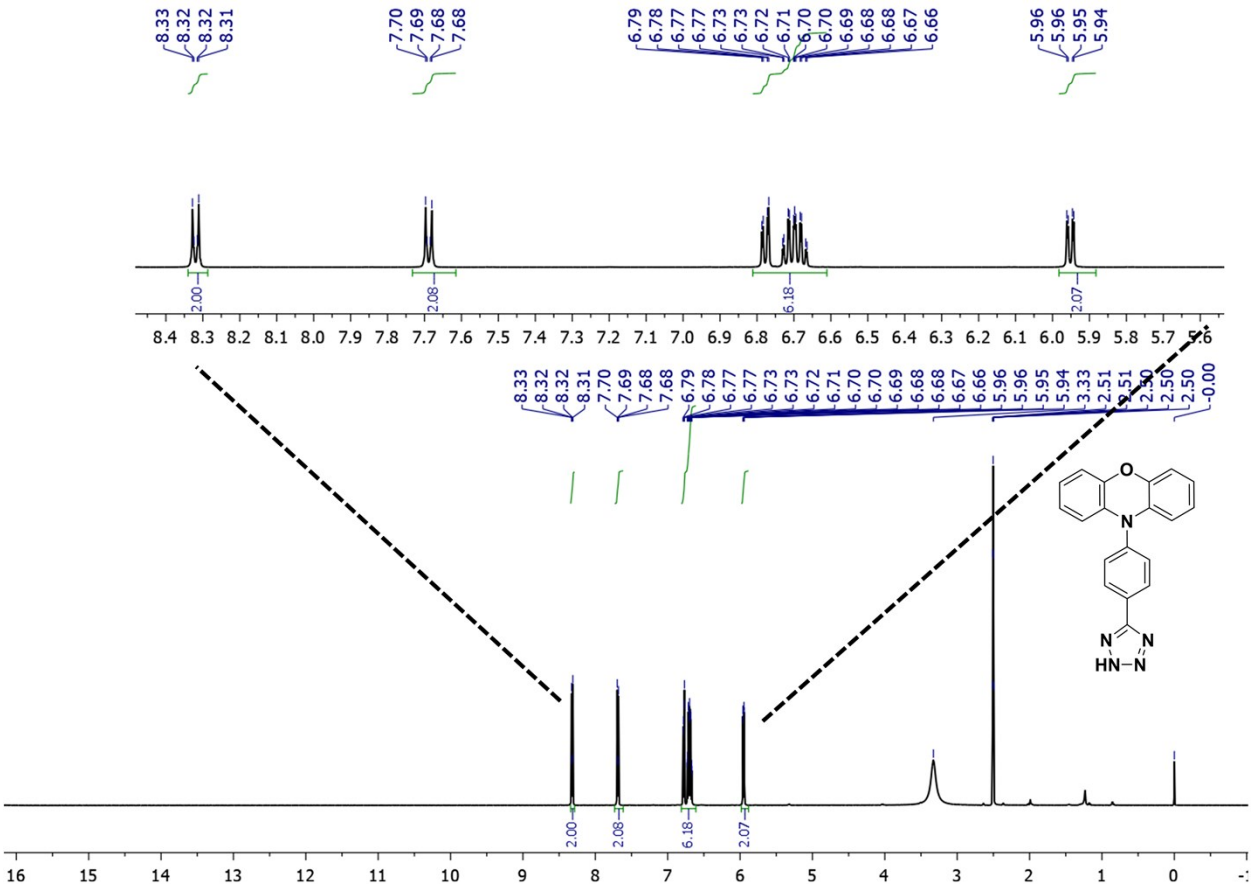

Figure S5. ^{1}H NMR spectrum of 10-(4-(2*H*-tetrazol-5-yl)phenyl)-10*H*-phenoxazine (**PXZ-TZ**)in DMSO-D_6 (500 MHz, 25 °C).

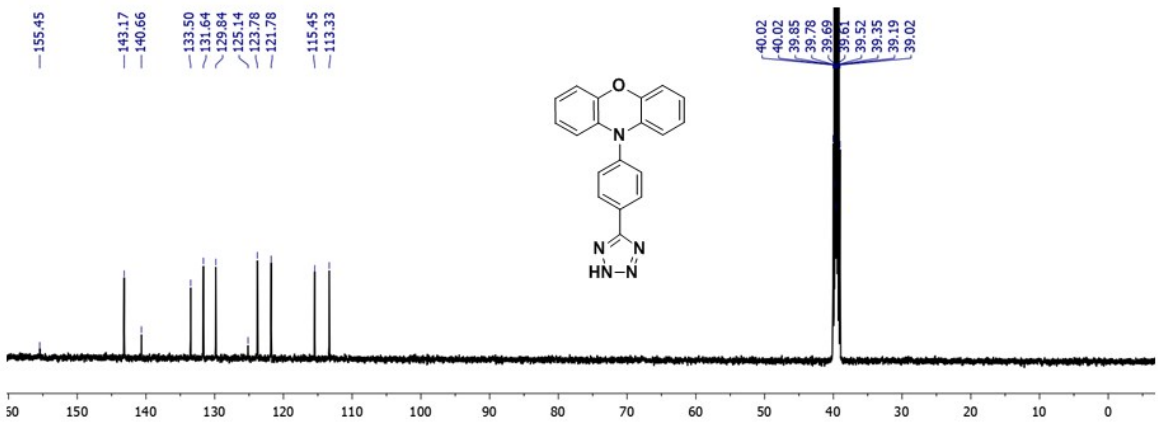

Figure S6. ^{13}C NMR spectrum of 10-(4-(2*H*-tetrazol-5-yl)phenyl)-10*H*-phenoxazine **(PXZ-TZ)** in DMSO-D_6 (125 MHz, 25 °C).

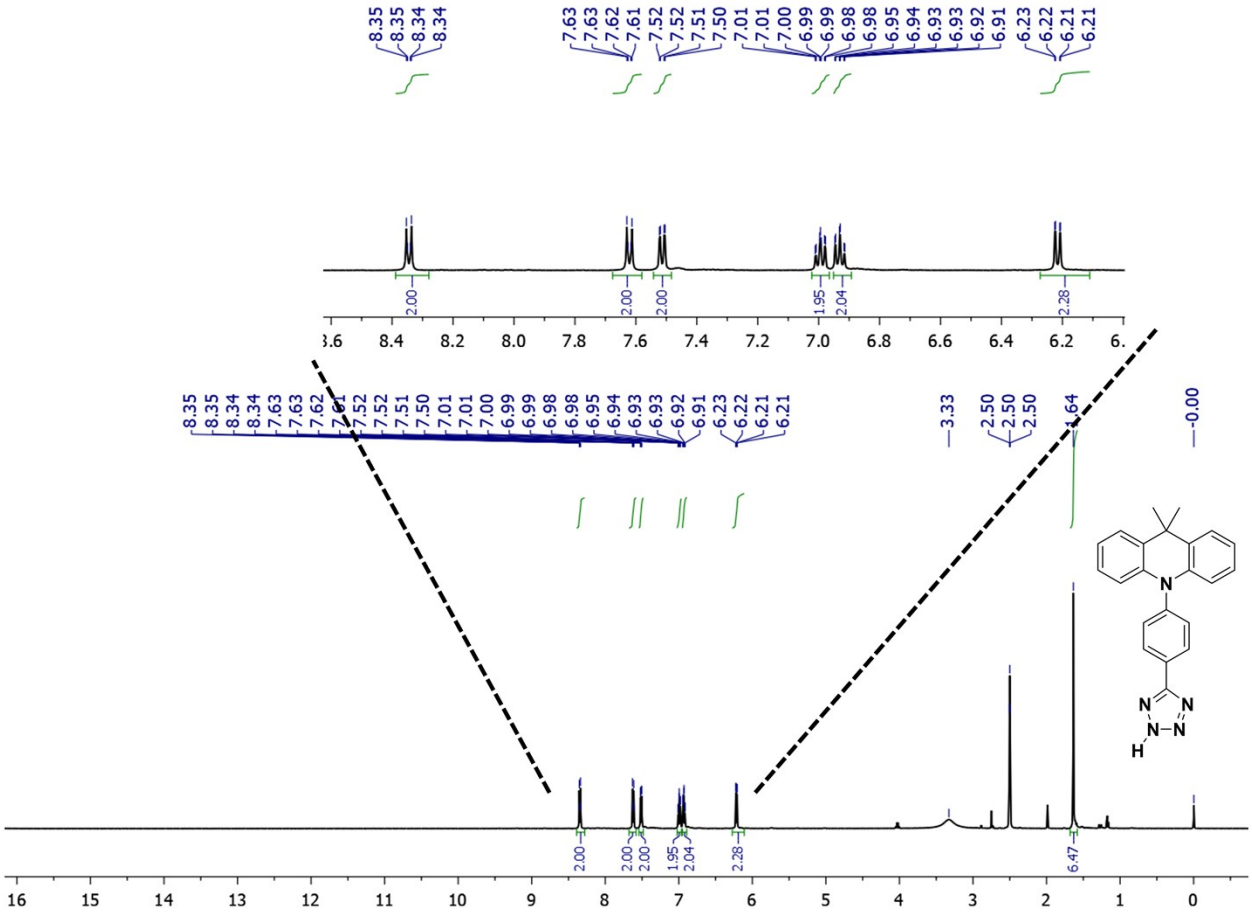

Figure S7. ^{1}H NMR spectrum of 10-(4-(2*H*-tetrazol-5-yl)phenyl)-9,9-dimethyl-9,10-dihydroacridine **(DMAC-TZ)** in DMSO-D_6 (500 MHz, 25 °C).

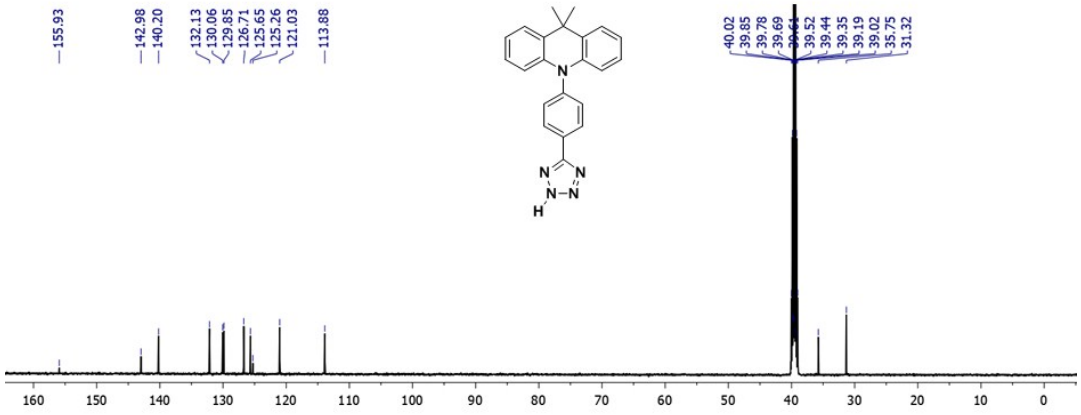

Figure S8. ^{13}C NMR spectrum of 10-(4-(2*H*-tetrazol-5-yl)phenyl)-9,9-dimethyl-9,10-dihydroacridine **(DMAC-TZ)** in DMSO-D_6 (125 MHz, 25 °C).

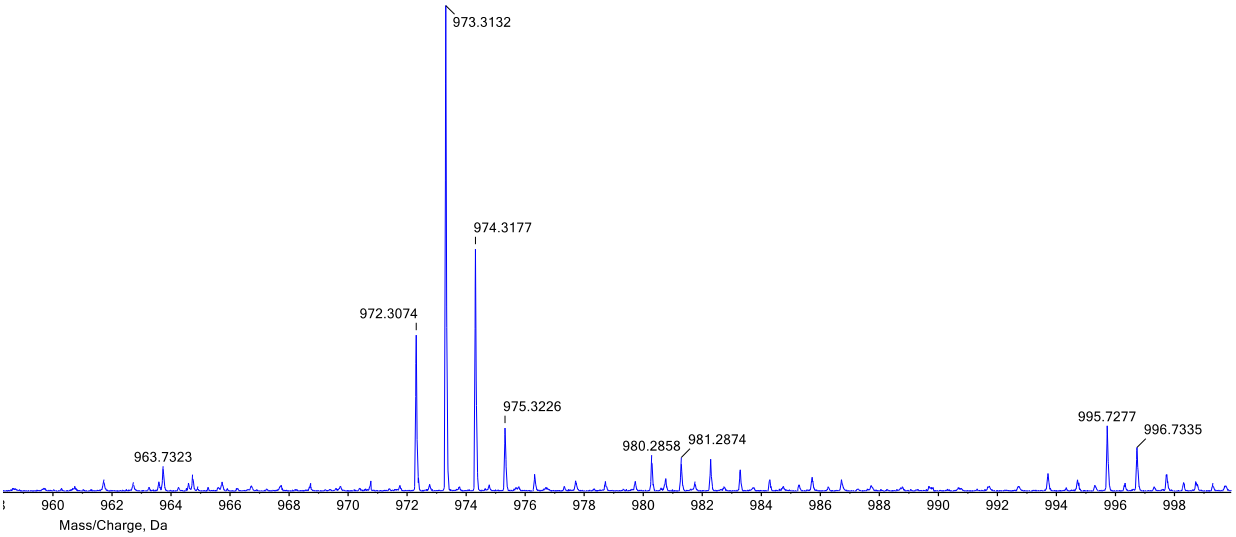

Figure S9. HRMS (ESI) spectrum of **TTT-PXZ**.

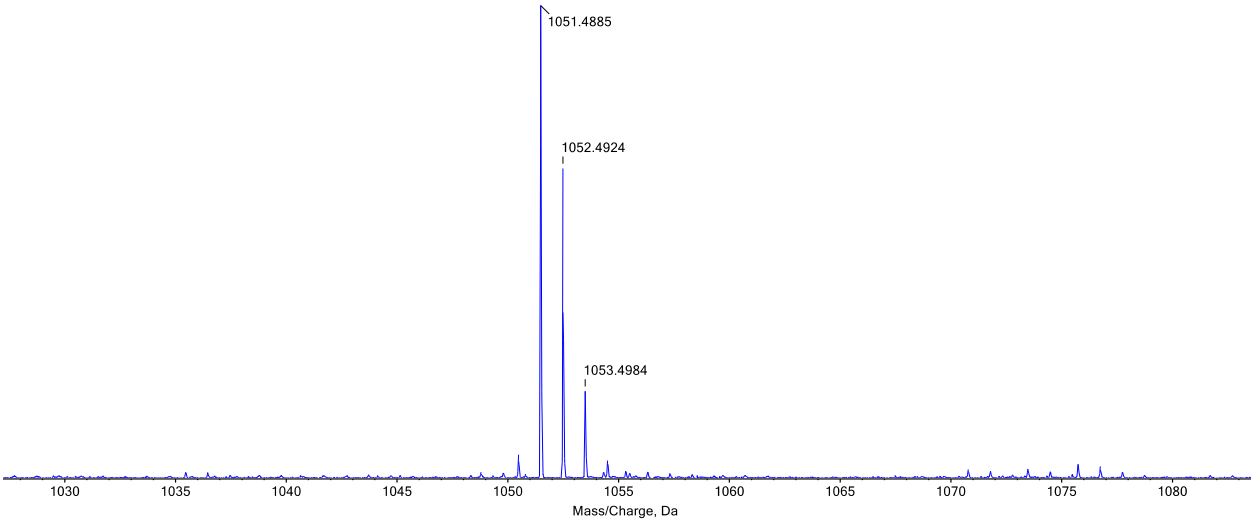

Figure S10. HRMS (ESI) spectrum of **TTT-DMAC**.

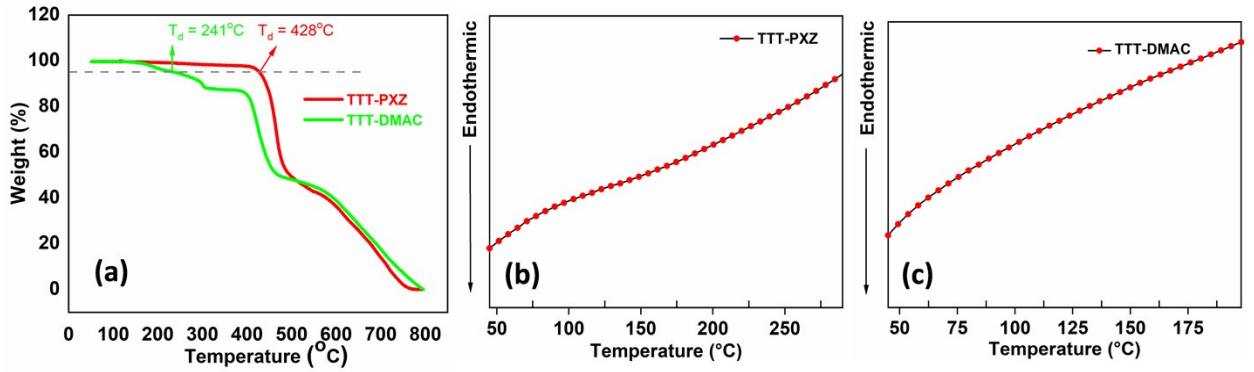

Figure S11. (a) TGA curve under N_2 with heating rate of 10 °C/min, (b) and (c) Second heating curve of compound **TTT-PXZ and TTT-DMAC** under N_2 with heating rate of 10 °C/min respectively.

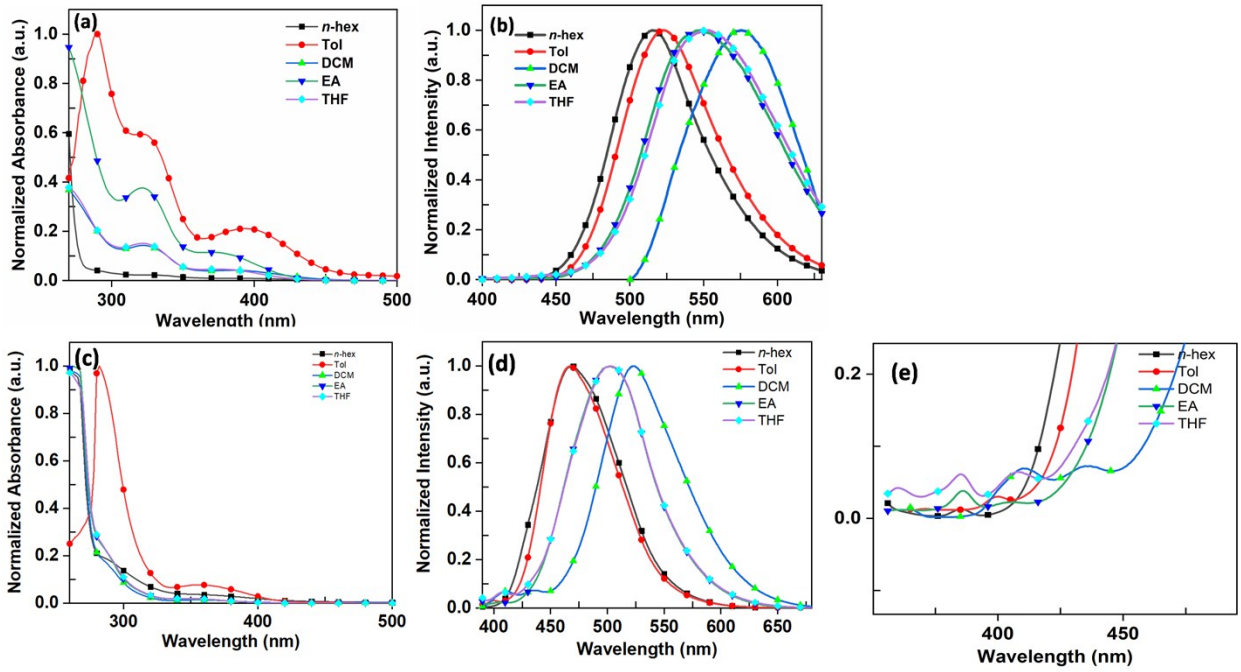

Figure S12. UV-Vis absorption spectra (a) and (c), fluorescence spectra (b)and (d) of **TTT-PXZ and TTT-DMAC** in different solvents respectively. (*n*-hex = *n*-hexane, Tol = toluene, DCM = dichloromethane, EA = ethyl acetate and THF = tetrahydrofuran, c = 1.0×10^{-5} M). (e) Magnification of Fig S12 (d) in the region 350-450 nm of **TTT-DMAC**.

Table S1 The emission peak of **TTT-PXZ** and **TTT-DMAC** in different solvents

Compound	λ/ nm (*n*-hex)	λ/ nm (Tol)	λ/ nm (THF)	λ/ nm (EA)	λ/ nm (DCM)
TTT-PXZ	515	522	550	548	575
TTT-DMAC	468	468	503	503	523

Table S2 The absorption and emission peak of **TTT-PXZ** and **TTT-DMAC** in toluene and spin coated film

Compound	$\lambda_{abs}{}^{a}$ (nm)	$\lambda_{PL}{}^{a}$(nm)	$\lambda_{abs}{}^{b}$ (nm)	$\lambda_{PL}{}^{b}$ (nm)
TTT-PXZ	291, 322, 394	522	242, 275, 331, 394	516
TTT-DMAC	290, 358	468	279, 364	478
[a] Measured in toluene (10^{-5} M) at room temperature. [b]Measured in spin coated films at room temperature				

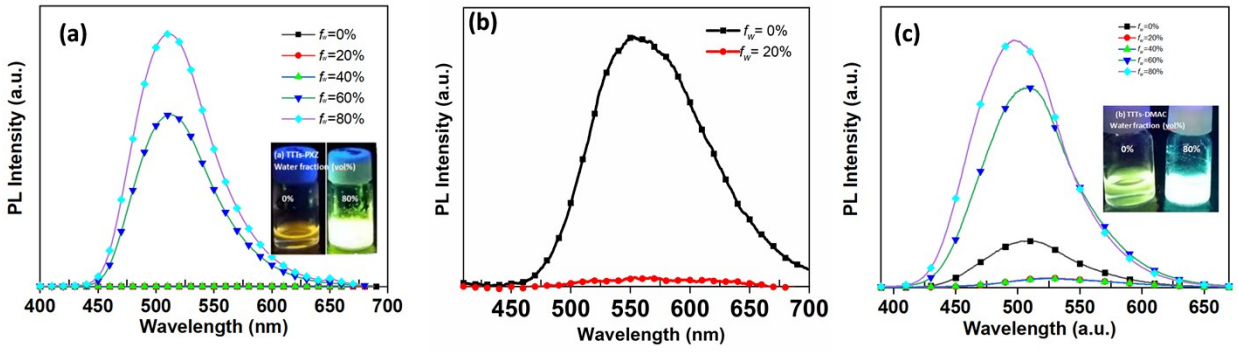

Figure S13. Photoluminescence (PL) spectra of (a) **TTT-PXZ** (b) magnification of PL spectra of **TTT-PXZ** and (c) **TTT-DMAC** in THF/water mixtures with different volume ratio of water (f_w).

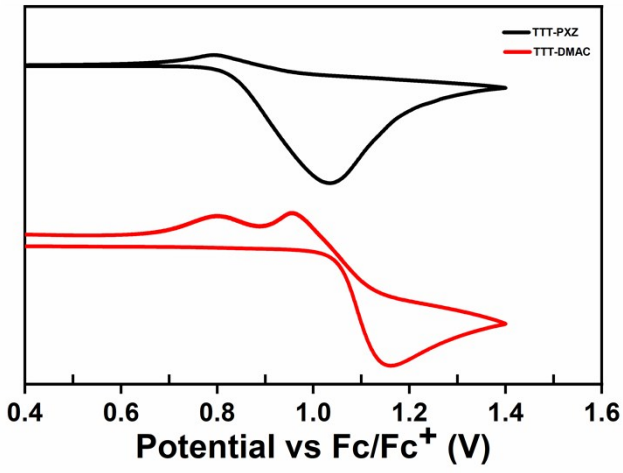

Figure S14. The cyclic voltammetry curves in acetonitrile of **TTT-PXZ** and **TTT-DMAC**.

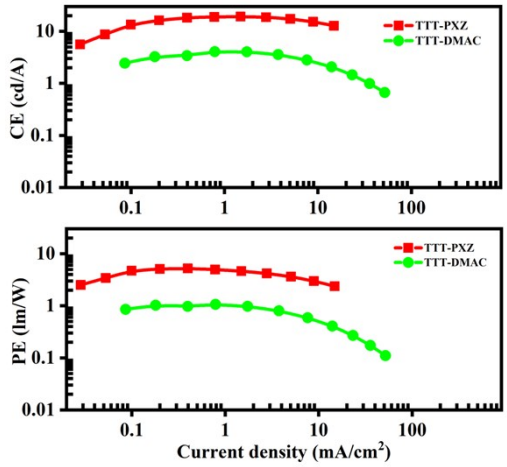

Figure S15. The current efficiency (a) and power efficiency (b) versus current density of device based on **TTT-PXZ** and **TTT-DMAC** emitters.

Exciton Lifetime and Rate Constant [1]

To calculate the rate constant of **TTT-PXZ**, the prompt PLQY (Φ_p) and delayed PLQY (Φ_d) were determined by using the total PLQY and the integrated intensity ratio between prompt and delayed components which was calculated from transient photoluminescence measurements. The intensity ratio between prompt (τ_p) and delayed (τ_d) components were determined using two fluorescent lifetimes (τ_p, τ_d) and fitting parameter (A_p, A_d) as follow.

$$I(t) = A_p e^{-1/\tau_p} + A_d e^{-1/\tau_d} \quad (1)$$

$$r_p = A_p\tau_p / (A_p\tau_p + A_d\tau_d) = 0.0884 \quad (2)$$

$$r_d = A_d\tau_d / (A_p\tau_p + A_d\tau_d) = 0.9116 \quad (3)$$

Then, the prompt PLQY (Φ_p) and delayed PLQY (Φ_d) were determined using intensity ratio (r_p, r_d) and total PLQY.

$$\Phi_{total} = \Phi_p + \Phi_d = 0.395 \quad (4)$$

$$\Phi_p = r_p\Phi_{total} = 0.0884 \times 0.395 = 0.035 \quad (5)$$

$$\Phi_d = r_d\Phi_{total} = 0.9116 \times 0.395 = 0.360 \quad (6)$$

The rate constants of ISC (k_{ISC}) and RISC (k_{RISC}) of **TTT-PXZ** emitter based on the following equations:

$$k_p = 1/\tau_p = 1 \div 36.2 \times 10^{-9} = 0.028 \times 10^9\ s^{-1} \quad (7)$$

$$k_d = 1/\tau_d = 1 \div 4.2 \times 10^{-6} = 0.238 \times 10^6\ s^{-1} \quad (8)$$

$$k_r = \Phi_p k_p + \Phi_d k_d \approx \Phi_p k_p = 0.035 \times 0.028 \times 10^9 = 0.098 \times 10^7\ s^{-1} \quad (9)$$

$$k_{RISC} \approx k_p k_d \Phi / k_r = [(0.028\times10^9\ s^{-1})(0.238 \times 10^6\ s^{-1})(0.395)] \div (0.098 \times 10^7\ s^{-1}) = 2.69 \times 10^6\ s^{-1} \quad (10)$$

$$k_{ISC} \approx k_p k_d \Phi_d / k_{RISC}\Phi_p = [(0.028\times10^9\ s^{-1})(0.238 \times 10^6\ s^{-1})(0.360)] \div [(2.69 \times 10^6\ s^{-1})\ 0.035] = 2.55 \times 10^7\ s^{-1} \quad (11)$$

Similarly, to calculate the rate constant of **TTT-DMAC**

$$r_p = A_p\tau_p / (A_p\tau_p + A_d\tau_d) = 0.0879 \quad (12)$$

$$r_d = A_d\tau_d / (A_p\tau_p + A_d\tau_d) = 0.9121 \quad (13)$$

Then, the prompt PLQY (Φ_p) and delayed PLQY (Φ_d) were determined using intensity ratio (r_p, r_d) and total PLQY.

$$\Phi_{total} = \Phi_p + \Phi_d \quad = 0.214 \qquad (14)$$

$$\Phi_p = r_p \Phi_{total} \quad = 0.0879 \times 0.214 = 0.019 \qquad (15)$$

$$\Phi_d = r_d \Phi_{total} \quad = 0.9121 \times 0.214 = 0.195 \qquad (16)$$

The rate constants of ISC (k_{ISC}) and RISC (k_{RISC}) of **TTT-DMAC** emitter based on the following equations:

$$k_p = 1/\tau_p \quad = 1 \div 49.5 \times 10^{-9} = 0.020 \times 10^9\ s^{-1} \qquad (17)$$

$$k_d = 1/\tau_d \quad = 1 \div 4.6 \times 10^{-6} = 0.217 \times 10^6\ s^{-1} \qquad (18)$$

$$k_r = \Phi_p k_p + \Phi_d k_d \approx \Phi_p k_p \quad = 0.019 \times 0.020 \times 10^9\ s^{-1} \qquad (19)$$

$$= 0.038 \times 10^7\ s^{-1}$$

$$k_{RISC} \approx k_p k_d \Phi / k_r = [(0.020 \times 10^9\ s^{-1})\ (0.217 \times 10^6\ s^{-1})\ (0.214)] \div (0.038 \times 10^7\ s^{-1}) \qquad (20)$$

$$= 2.44 \times 10^6\ s^{-1}$$

$$k_{ISC} \approx k_p k_d \Phi_d / k_{RISC} \Phi_p = [(0.020 \times 10^9\ s^{-1})\ (0.217 \times 10^6\ s^{-1})\ (0.195)] \div [(2.44 \times 10^6\ s^{-1})\ 0.019] \qquad (21)$$

$$= 1.83 \times 10^7\ s^{-1}$$

References

1. J. Li, W. -C. Chen, H. Liu, Z. Chen, D. Chai, C.-S. Lee, C. Yang, *J. Mater. Chem. C*, 2020, 8, 602-606.